INTERNATIONAL JOURNAL OF PRECISION ENGINEERING AND MANUFACTURING Vol. 16, No. 6, pp. 1067-1074

DOI: 10.1007/s12541-015-0138-6
ISSN 2234-7593 (Print) / ISSN 2005-4602 (Online)

A Fuzzy-P Controller of an Active Reaction Force Compensation (RFC) Mechanism for a Linear Motor Motion Stage

Duc Canh Nguyen[1] and Hyeong-Joon Ahn[2,#]

1 Department of Mechanical Engineering, Graduate School, Soongsil University, 369 Sangdo-ro, Dongjak-gu, Seoul, 156-743, South Korea
2 Department of Mechanical Engineering, Soongsil University, 369 Sangdo-ro, Dongjak-gu, Seoul, 156-743, South Korea
Corresponding author / E-mail: ahj123@ssu.ac.kr, TEL: +82-2-820-0654, FAX: +82-2-820-0668

KEYWORDS: Active reaction force compensation, Linear motor motion stage, Fuzzy-P controller

Residual vibration of system base due to high-speed motion of a stage may significantly reduce life span and productivity of the manufacturing equipment. Although a passive reaction force compensation (RFC) mechanism was developed to reduce residual vibration of a linear motor motion stage, the passive RFC mechanism should be redesigned according to variation of motion profiles. In this paper, we develop a fuzzy-P (proportional) controller of an active RFC mechanism to automatically tune the gain according to variation of motion profiles. First, frequency components of motion profiles for a linear motion stage are analyzed and performances of the passive RFC mechanism are approximately evaluated using a motion profile analysis. An active RFC mechanism with an additional control coil is introduced to overcome limitation of the passive RFC mechanism and a fuzzy rule is proposed to automatically tune the P controller of the active RFC mechanism according to variations of motion profiles. Simulations and experiments are performed to show effectiveness of the proposed fuzzy rule for tuning the P control gain of the active RFC mechanism.

Manuscript received: November 25, 2014 / Revised: March 28, 2015 / Accepted: April 7, 2015

NOMENCLATURE

a_M = acceleration of mover
c_{MT} = damping of magnet track
k_{MT} = stiffness of magnet track
k_v = viscous friction of mover
k_P = gain of P control
F_f = thrust force for mover friction
F_{fc} = Column friction of mover
F_{fs} = Stribeck friction of mover
F_m = thrust force for mover motion
F_t = thrust or reaction force
F_{tran} = transmitted force
m_M = mass of mover
m_{MT} = mass of magnet track
n = index of frequency component
n_s = Stribeck friction coefficient for exponential function
n_{max} = index of frequency component at peak acceleration of mover
n_{MT} = index of natural frequency of magnet track
n'_{MT} = output of defuzzification block
T = period of motion profile
T_a = acceleration time
T_{dw} = dwell time
T_r = run time
v_s = Stribeck friction coefficient for velocity
x_{MT} = position of magnet track
$\dot{x}_{MT}$ = velocity of magnet track
$\ddot{x}_{MT}$ = acceleration of magnet track
ω = frequency
ω_{MT} = natural frequency of magnet track
ω_T = fandamental frequency of motion profile
ζ = damping ratio
θ_n = phase of magnet track motion

Springer

1. Introduction

Demand for a motion stage with high-speed and high precision is fastly growing as the productivity of semi-conductor and display panel industries are rapidly promoted.[1] In particular, semi-conductor lithography systems require both extreme precision and high speed in very long stroke such sub-nanometer accuracy and 230 wafers/hour over 2 m stroke.[2]

Residual vibration of system base due to high-speed motion of a linear motion stage may reduce life span and productivity of manufacturing equipment. Rapid acceleration or deceleration motion of the stage induces large reaction force, which causes the system base to oscillate either with considerable amplitude or in substantially long settling time. In particular, vibration problem of a motion stage becomes more important issue since its moving mass and working area increase with enlarged size of display or wafer.

Base vibration of a linear motor motion stage has been reduced with a passive reaction force compensation (RFC) mechanism.[3] The RFC mechanism is installed into the linear motor and does not require any additional external structure or motor, so that we can make the system very compact. Only a part of the reaction force (force of spring and damper of the magnet track) is transmitted into the system base while inertial force of the magnet track is dissipated during its own oscillation.[4,5] However, dummy mass and spring of the magnet track should properly be adjusted according to the motion profiles in order for reduction of the base vibration.

Active RFC mechanisms for a linear motion stage were introduced to overcome the limitation of passive RFC mechanisms.[6,7] A dummy motion axis is added to the system and generates a counter force to cancel out the reaction force. However, the system needs double the power and double the space.

An additional control coil can reduce the reaction force of a linear motor motion stage against motion profile variations. Spring and damping coefficients (or gains of PD control) of the magnet track can be adjusted with the control coil. However, control gains highly depend on the motion profiles and should be tuned appropriately according to variation of motion profiles. In addition, it is very difficult to know optimal gains with an analytical method since the motion profiles for a linear motion stage are periodic functions and has numerous frequency components.[5]

Fuzzy logic is a rule-based decision making method using heuristic thinking process of human beings.[8] Fuzzy logic is suitable for industrial process controls that a human controlled manually with experiential expertise.[9] Linguistic control rules of a human expert can be directly translated to a rule base fuzzy logic control. Especially, conventional PID controls were improved with fuzzy logic for robust performance to uncertainties or nonlinearities.[10-12]

In this paper, we present a fuzzy-P (proportional) controller of an active RFC mechanism to automatically tune the gain according to variation of motion profiles. First, motion profiles for a linear motion stage are analyzed using Fourier series and responses of the passive RFC mechanism are approximately evaluated using the motion profile analysis. An active RFC mechanism with an additional control coil is introduced to overcome limitation of the passive RFC mechanism and a fuzzy rule is proposed to automatically adjust P gain of the active RFC mechanism according to variations of the motion profile. Simulations and experiments show that the proposed fuzzy rule is very effective for automatically tuning the P control gain of the active RFC.

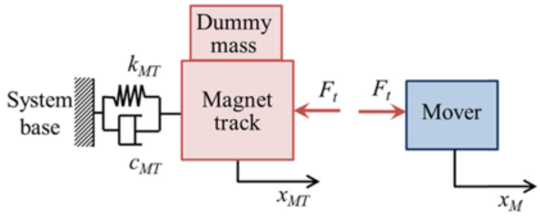

Fig. 1 Schematic of the passive RFC mechanism

2. Passive RFC Mechanism

Fig. 1 shows a schematic of the passive RFC mechanism.[3] When the mover moves due to thrust force (F_t), its reaction force makes the magnet track (m_{MT}) oscillate and creates displacement (x_{MT}) since the magnet track is supported by spring (k_{MT}) and damper (c_{MT}).

Equation of motion of the passive RFC mechanism is given by Eq. (1).[3] The thrust or reaction force (F_t) consists of two main parts: force for the mover acceleration and force against friction of the mover.

$$m_{MT}\ddot{x}_{MT}+c_{MT}\dot{x}_{MT}+k_{MT}x_{MT}=F_t \tag{1}$$

The transmitted force to the system base is expressed with Eq. (2). The reaction force (F_t) is divided into the inertial force of the magnet track ($m_{MT}\ddot{x}_{MT}+c_{MT}\dot{x}_{MT}+k_{MT}x_{MT}=F_t$) and the transmitted force (F_{tran}) to the system base.

$$F_{tran}=c_{MT}\dot{x}_{MT}+k_{MT}x_{MT} \tag{2}$$

Transfer functions from thrust force to the magnet track displacement and to the transmitted force are Eqs. (3) and (4), respectively.

$$\left\|\frac{x_{MT}(\omega)}{F_t(\omega)}\right\|=\left|\frac{1}{-m_{MT}\omega^2+jc_{MT}\omega+k_{MT}}\right| \tag{3}$$

$$\left\|\frac{F_{tran}(\omega)}{F_t(\omega)}\right\|=\left|\frac{jc_{MT}\omega+k_{MT}}{-m_{MT}\omega^2+jc_{MT}\omega+k_{MT}}\right| \tag{4}$$

Frequency analysis of the motion profile is inevitable to predict performance of the passive RFC mechanism since two transfer functions of Eqs. (3) and (4) depend on excitation frequency of thrust force F_t. Therefore, both stiffness and damping of the magnet track should be adjusted according to the variation of motion profiles.

3. Analysis of Motion Profile using Fourier Series

3.1 Classification of motion profiles

There are repetitive motion profiles used in a linear motor motion stage such as ping-pong (back and forth) motion, repetitive go-and-stop motion and combined motions. Fig. 2(a) shows a long stroke ping-pong

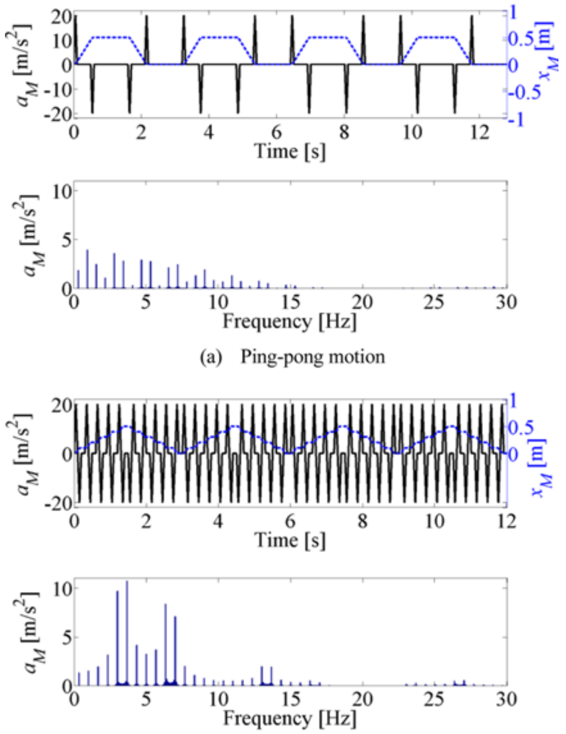

(a) Ping-pong motion

(b) Repetative go-and-stop motion

Fig. 2 Example motion profiles[4]

motion (accleration time T_a is 0.05s, run time T_r is 0.4s, dwell time T_{dw} is 1s and peak acceleration is 20 m/s^2) and its frequency components. On the other hand, Fig. 2(b) shows a repetitive go-and-stop motion (accleration time T_a is 0.1s, run time T_r is 0s ,dwell time T_{dw} is 0.1s and peak acceleration is 20 m/s^2) and its frequency components. Although the total stroke of both motion profiles are same, frequency components of two motion profiles are totally different.

3.2 Motion profile analysis

In this paper, we focus on the long stroke ping-pong motion since a long stroke motion is more important than a short stroke motion.[4]

The long stroke motion can be modeled mathematically using several time constants: T_a is acceleration time, T_r is run time and T_{dw} is dwell time, as shown in Fig. 3. Period of the ping-pong motion is $T = 4T_a + 2T_r + 2T_{dw}$. The acceleration time T_a is set to be 0.1 s for maximum acceleration (20 m/s^2) with a given peak thrust force of the linear motor. The run time (T_r) is related to the stroke of the motion profile. If T_r is long, the motion profile is called by a long stroke motion, as shown in Fig. 2(a). On the other hand, if T_r is short, the motion profile is called by a short stroke motion, as shown in Fig. 2(b). The run time is limited by size of the motion stage and is assumed to be smaller than 0.6 s. The dwell time varies according to requirements of the manufacturing device and is assumed not to be greater than 2 s.

Frequency components of the motion profile can be calculated with Fourier series. According to Fourier series, any periodic function $a_M(t)$ with period T can be represented with Eq. (4).

$$a_M(t) = \frac{a_0}{2} + \sum_{n=1}^{\infty}(a_n\cos(n\omega_T t) + b_n\sin(n\omega_T t)) \quad (4)$$

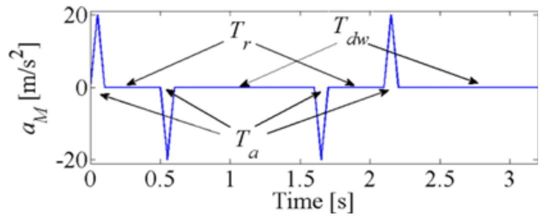

Fig. 3 Acceleration of the ping-pong motion

where $a_0 = \frac{2}{T}\int_0^T a_M(t)dt$, $a_n = \frac{2}{T}\int_0^T a_M(t)\cos(n\omega_T t)dt$, and $b_n = \frac{2}{T}\int_0^T a_M(t)\sin(n\omega_T t)dt$

The motion profile is shifted by $T_{dw}/2$ so that a_M becomes an even function and the coefficients b_n become zeros. Fourier coefficient a_n can be derived as Eq. (5).

$$a_n = \frac{4A_{max}T_a}{T}\sin\left(\frac{\pi n}{2}\right)\sin\left(\pi n\frac{T_a+T_r}{T}\right)\frac{\sin^2\left(\pi n\frac{T_a}{2T}\right)}{\left(\pi n\frac{T_a}{2T}\right)^2} \quad (5)$$

We can approximate n_{max} as Eq. (6) so that a_n becomes maximum. The Fourier coefficient a_n has maximum value ($4A_{max}T_a/T$) when all three sine functions have maximal values. The first sine function becomes one when n is odd. In addition, the last sine function becomes one if n is small and T_a is much smaller than T. Furthermore, the last sine function decreases exponentially as n increases.

$$n_{max} \approx 1 + \left[\frac{T_a+T_{dw}}{T_a+T_r}\right]_{2k} = 1, 3, 5, \ldots \quad (6)$$

3.3 Reponses of passive RFC mechanism

The particular solution $x_{MT}(t)$ of Eq. (1) due to the reaction force can be obtained with Eq. (7). In this section, in order for simple analysis, we consider only the thrust force for the mover accleration.

$$m_{MT}\ddot{x}_{MT} + c_{MT}\dot{x}_{MT} + k_{MT}x_{MT} = m_M\left(\frac{a_0}{2} + \sum_{n=1}^{\infty}a_n\cos(n\omega_T t)\right) \quad (7)$$

where, ω_T ($=2\pi/T$) is fundamental frequency of the motion profile:

The n^{th} particular solution of Eq. (7) can be given in Eq. (8).

$$x_{MT}^{(n)}(t) = \frac{a_n m_M}{m_{MT}[(\omega_{MT}^2-(n\omega_T)^2)^2+(2\zeta\omega_{MT}n\omega_T)^2]^{1/2}}\cos(n\omega_T t - \theta_n) \quad (8)$$

where,

$$\omega_{MT} = \sqrt{\frac{k_{MT}}{m_{MT}}},\ \zeta = \frac{c_{MT}}{2\sqrt{k_{MT}m_{MT}}},\ \theta_n = \tan^{-1}\frac{2\zeta\omega_{MT}n\omega_T}{\omega_{MT}^2-(n\omega_T)^2}$$

and n_{MT} is an index of natural frequency of the magnet track.

The stiffness of the magnet track (k_{MT}) should be chosen to minimize the transmitted force ($F_{tran}=c_{MT}\dot{x}_{MT}+k_{MT}x_{MT}$) under condition that the magnet track motion (x_{MT}) is less than a certain value such as 0.1 m. Although a damper can be used to avoid resonance of the passive RFC, it will increase the transmitted force on the system base.[4] If natural frequency of the magnet track is assumed as $\omega_{MT} = n_{MT}\omega_T$ and the

Table 1 Heuristic guide line for n_{MT}

n_{MT}	Reference parameter	Performance	
		F_{tran}	x_{MT}
Even	-	↓	↓
n_{MT} ↓	-	↓	↑
$\vert n_{MT}-n_{max}\vert$ ↑	$n_{max}\approx 1+\left[\frac{T_a+T_{dw}}{T_a+T_r}\right]_{2k}$	↓	↓
T ↑	$T=4T_a+2T_r+2T_{dw}$	↓	↑

damping is assumed to be zero for simplicity, the magnitude of the n^{th} particular solution can be written as Eq. (9).

$$\left\|x_{MT}^{(n)}\right\| = \frac{m_M}{m_{MT}\pi^2}\frac{A_{max}T_aT}{\left|n_{MT}^2-n^2\right|}\sin\left(\frac{\pi n}{2}\right)\sin\left(\pi n\frac{T_a+T_r}{T}\right)\frac{\sin^2\left(\pi n\frac{T_a}{2T}\right)}{\left(\pi n\frac{T_a}{2T}\right)^2} \tag{9}$$

From Eqs. (6) and (9), the largest component of particular x_{MT} is:

$$\left\|x_{MT}^{(n)}\right\| = \frac{m_M}{m_{MT}\pi^2}\frac{A_{max}T_aT}{\left|n_{MT}^2-n^2\right|}\sin\left(\frac{\pi n}{2}\right)\sin\left(\pi n\frac{T_a+T_r}{T}\right)\frac{\sin^2\left(\pi n\frac{T_a}{2T}\right)}{\left(\pi n\frac{T_a}{2T}\right)^2} \tag{10}$$

In addition, magnitude of the transmitted force due to the n^{th} particular solution of x_{MT} can be derived as Eq. (11) and corresponding stiffness of the magnet track is shown in Eq. (12).

$$\left\|F_{tran}\right\|^{(n)} = k_{MT}\left\|x_{MT}\right\|^{(n)} \tag{11}$$

$$k_{MT} = m_{MT}\omega_{MT}^2 = m_{MT}\frac{4\pi^2n_{MT}^2}{T^2} \tag{12}$$

The largest component of the particular transmitted force F_{tran} can be calculated from the largest component of x_{MT}:

$$\left\|F_{tran}\right\|^{(n_{max})} = k_{MT}\left\|x_{MT}\right\|^{(n_{max})} = m_M\frac{n_{MT}^2}{\left|n_{MT}^2-n_{max}^2\right|}\frac{4A_{max}T_a}{T} \tag{13}$$

We can deduce some heuristic guide lines for n_{MT}, as shown in Table 1 since the largest component of the transmitted force $\left\|F_{tran}\right\|^{(n_{max})}$ should be minimized in order to reduce the total transmitted force. The stiffness of the magnet track (n_{MT}) should be chosen according to the motion profile.

4. Fuzzy-P Controller for the Active Coil

4.1 Active RFC mechanism with P controller

A schematic of the active RFC with P controller is shown in Fig. 4. Equation of motion of the active RFC with active coil is shown in Eq. (14).

$$m_{MT}\ddot{x}_{MT}+c_{MT}\dot{x}_{MT}+k_{MT}x_{MT}=F_t \tag{14}$$

Only P controller is used to both regulate the motion of the magnet track and minimize the transmitted force as Eq. (15) since damping reduces vibration of the magnet track near resonance but increases transmitted force in entire frequency range.

$$F_{tran}=c_{MT}\dot{x}_{MT}+k_Px_{MT} \tag{15}$$

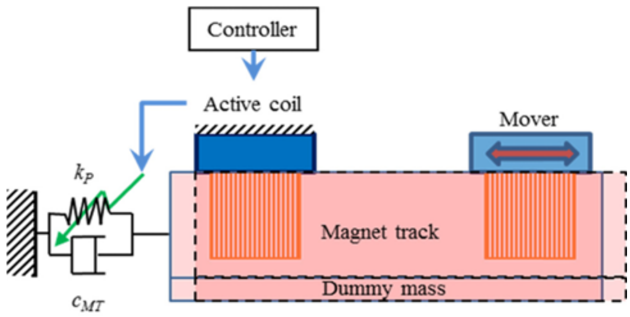

Fig. 4 Schematic of the active RFC with P controller

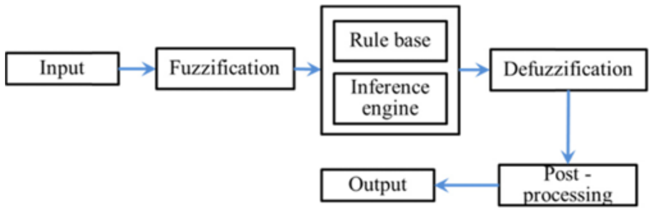

Fig. 5 Architecture of a fuzzy system

A motion equation of the active RFC with P controller can be rewritten as Eq. (16). From Eqs. (15) and (16), P gain (k_P) of the active RFC has a same role as stiffness of the passive RFC mechanism.

$$m_{MT}\ddot{x}_{MT}+c_{MT}\dot{x}_{MT}+k_Px_{MT}=F_t \tag{16}$$

4.2 Fuzzy-P controller

4.2.1 Fuzzy logic system

A fuzzy logic model is a mathematical procedure based on an "IF-THEN" rule system that mimics the way of human thinking in computational form.[13,14] Normally, a fuzzy system includes four modules (Fuzzification, Fuzzy inference, Rule base and Defuzzification), as shown in Fig. 5.

4.2.2 Active RFC with Fuzzy-P logic controller

Although the transmitted force and the magnet track motion of the passive RFC mechanism have a complex relationship with motion profiles, we can set up a rule for the stiffness of the magnet track to minimize the transmitted force under the condition that the magnet track motion is smaller than 0.1 m.

A schematic diagram of the active RFC with fuzzy-P control is shown in Fig. 6. Fuzzy logic is applied to choose the stiffness of the magnet track (gain k_P of the P controller). The fuzzy logic is developed using the fuzzy logic designer in Matlab-Simulink.[15] Two input variables (run time (T_r=0-0.6 s) and dwell time (T_{dw}=0-2 s)) and one output n'_{MT} are converted into linguistic variable (small = S, small-normal = SN, normal = N, normal-large = NL, large = L) by triangular membership functions, as shown in Fig. 7(a), (b) and (c).

Base on the motion profile analysis, heuristic rules can be derived and shown in Table 2. If T_r is small, constraint of the magnet track motion can easily be satisfied. Therefore, we can choose stiffness of the magnet track as small as possible, as shown in Table 2(a). If T_r is

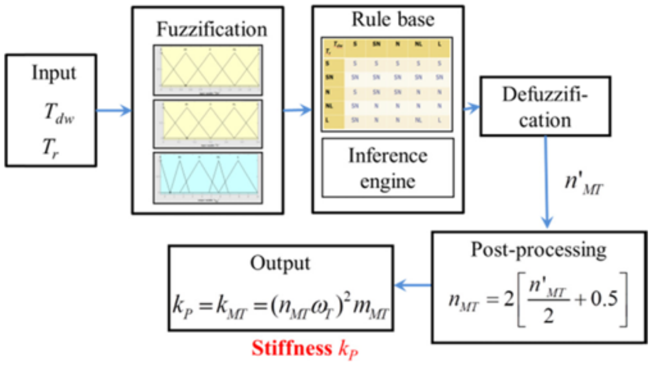

Fig. 6 Active RFC with fuzzy-P system

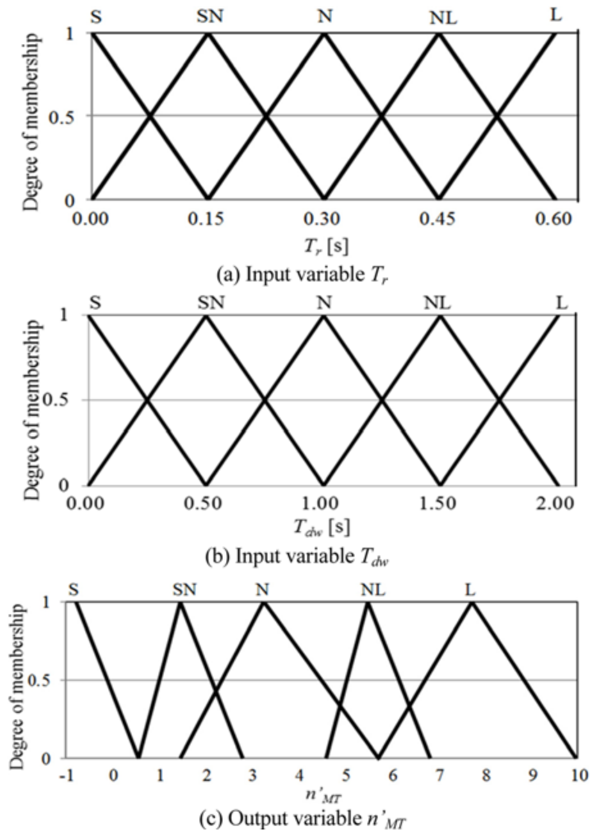

Fig. 7 Triangular membership functions of the fuzzy logic system

normal, the magnet track motion should be considered rather than the transmitted force and we have to increase n_{MT} according to the increase of T_r as shown in Table 2(b). If T_r is large, constraint of the magnet track motion should carefully be investigated and we should enlarge n_{MT} further as T increases, as shown in Table 2(c).

The fuzzy rules are summarized in Table 3. Here, max-min type decomposition is used and output of the fuzzy logic system is calculated based on the center of area gravity method.[13]

After the defuzzification, output from the fuzzy logic system (n_{MT}) should be chosen through a post-processing of Eq. (17), which guarantees that n_{MT} is the nearest even integer to the output and also confirms stiffness of the magnet track is large enough so that the magnet track motion is smaller than 0.1 m.

Table 2 Derived Fuzzy rule

(a) When T_r is N (≈ 0 s)				
Input variables		Intermediate parameters		Result
T_r	T_{dw}	$\Delta f = 1/T$	n_{max}	n_{MT}
S	S (≈0s)	L	N	S
S	N (≈1s)	NL	NL	S
S	L (≈2s)	NS	L	S
(b) T_r is N (≈ 0.3 s)				
Input variables		Intermediate parameters		Result
T_r	T_{dw}	$\Delta f = 1/T$	n_{max}	n_{MT}
N	S (≈0s)	L	S	S
N	N (≈1s)	N	N	SN
N	L (≈2s)	NS	NL	N
(c) T_r is N (≈ 0.6 s)				
Input variables		Intermediate parameters		Result
T_r	T_{dw}	$\Delta f = 1/T$	n_{max}	n_{MT}
L	S (≈0s)	NL	S	SN
L	N (≈1s)	N	N	N
L	L (≈2s)	S	L	L

Table 3 IF-THEN rule base for fuzzy logic system

T_r \ T_{dw}	S	SN	N	NL	L
S	S	S	S	S	S
SN	S	SN	SN	SN	SN
N	S	SN	SN	N	N
NL	SN	N	N	N	N
L	SN	N	N	NL	L

Table 4 Parameters of the passive RFC mechanism for simulation

Parameter	Value	Parameter	Value
m_{MT}	21 kg	F_{fc}	1N
k_{MT}	1200 N/m	F_{fs}	6N
c_{MT}	37 Ns/m	n_s	0.01
k_v	30 Ns/m	v_s	0.1

$$n_{MT} = 2\left[\frac{n'_{MT}}{2} + 0.5\right] \quad (17)$$

5. Simulation Results

5.1 Passive RFC with various motion profiles

A mathematical model of the passive RFC considering friction is shown in Eq. (18). Here, F_m is the thrust force for the mover motion or motion profile itself (product of mass of the mover and acceleration of the motion profile) and F_f is required force due to friction and cables of the mover (Eq. (19)). Guide friction of the magnet track is approximated as viscous damper since the magnet track is supported by a linear guide with low friction and low precision.

$$m_{MT}\ddot{x}_{MT} + c_{MT}\dot{x}_{MT} + k_{MT}x_{MT} = F_m + F_f \quad (18)$$

$$F_f(\dot{x}_M) = F_{fc}\,\mathrm{sgn}(\dot{x}_M) + F_{fs}\,e^{-n_s\left|\frac{\dot{x}_M}{v_s}\right|}\mathrm{sgn}(\dot{x}_M) + k_v\dot{x}_M \quad (19)$$

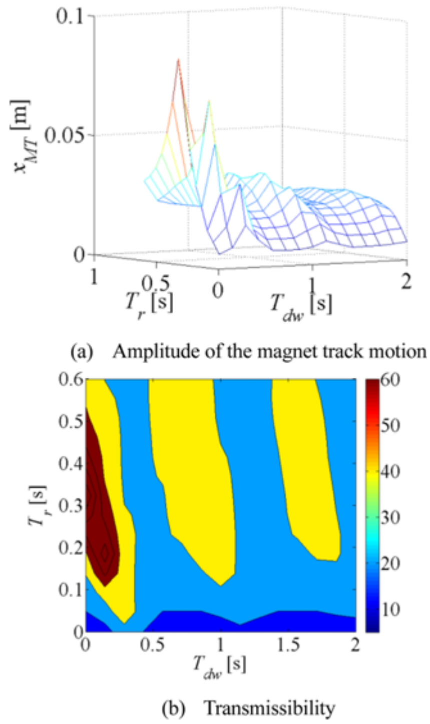

(a) Amplitude of the magnet track motion

(b) Transmissibility

Fig. 8 Simulations of the passive RFC with k_{MT} = 1200 N/m

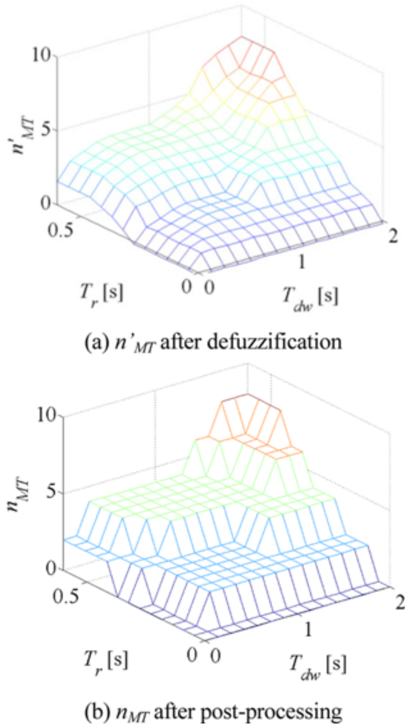

(a) n'_{MT} after defuzzification

(b) n_{MT} after post-processing

Fig. 9 Output of the fuzzy logic system

Here, F_c is Coulomb friction and F_s, n_s, v_s are Stribeck friction coefficients.

All parameters of the passive RFC mechanism for simulation are identified experimentally and are shown in Table 4. Detail procedure of the identification is out of scope of this paper.

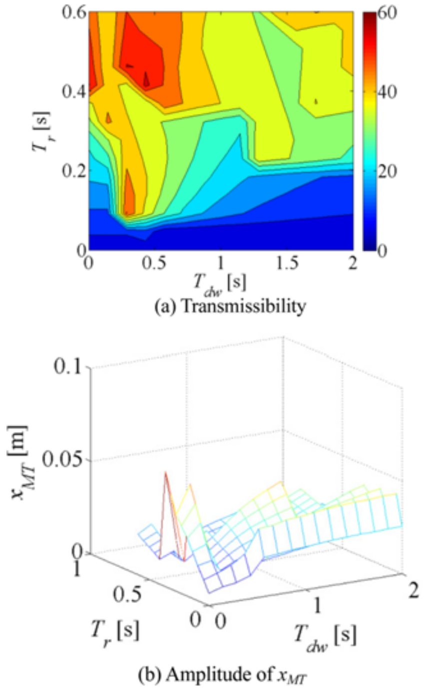

(a) Transmissibility

(b) Amplitude of x_{MT}

Fig. 10 Simulations of the active RFC with fuzzy-P control

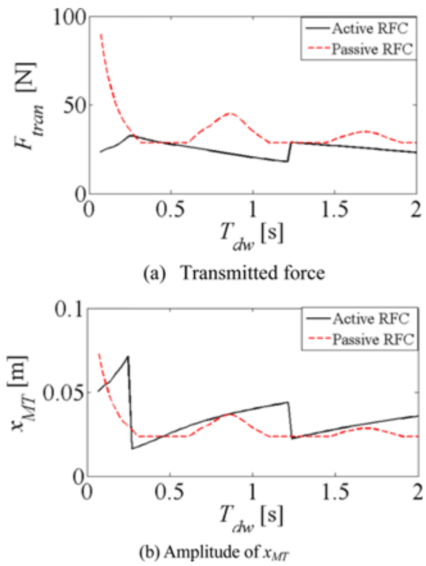

(a) Transmitted force

(b) Amplitude of x_{MT}

Fig. 11 Simulations of passive and active RFC's with T_r = 0.2769 s

Simulated transmissibility (amplitude of transmitted force over amplitude of reaction force) and amplitude of magnet track of the passive RFC mechanism are shown in Fig. 8 (k_{MT} = 1200 N/m). Since the passive RFC mechanism cannot adjust the stiffness of the magnet track according to the motion profiles, they cannot avoid the resonance of the magnet track and guarantee minimal transmitted force. We can clearly see resonance of the magnet track for small T_{dw} values.

5.2 Proposed active RFC with fuzzy-P controller

Raw and post-processed outputs of the proposed fuzzy logic system are shown in Fig. 9. The output increases as the run and dwell times

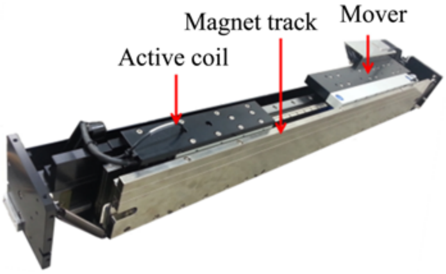

Fig. 12 Linear motor stage with active RFC mechanism

Table 5 Specifications of the linear motion stage

Liner motion stage	Peak/cont. force	810/240 N
	Resolution	1.0 µm
	Stroke	517 mm
	Maximum speed	5.0 m/s
Active coil	Peak/cont. force	416/104 N
	Hall sensor resolution	100 µm

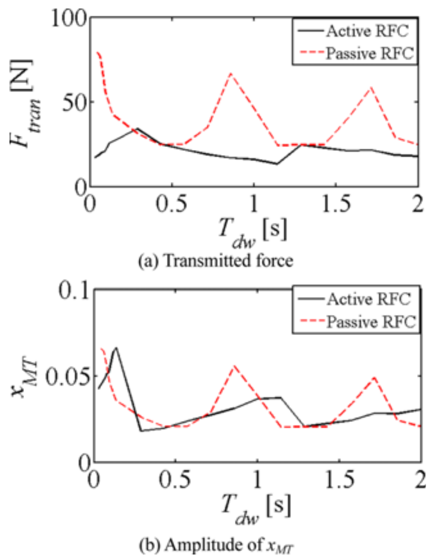

Fig. 13 Experiments of passive and active RFC's with T_r = 0.2769 s

increase. In addition, the output varies discontinuous since the output become integer after the post-processing.

Transmitted force and amplitude of the magnet track motion for the active RFC with the proposed fuzzy-P controller is shown in Fig. 10. The active RFC can avoid resonance and reduce the transmissibility about 60% in most regions compared to the passive RFC.

Simulation results of both RFC's with T_r = 0.2769 s and various T_{dw} are shown Fig. 11. In the entire range of T_{dw}, the active RFC maintains lower transmitted force than the passive RFC as satisfying the requirements of the magnet track motion (x_{MT} < 0.1 m).

6. Experiment

A linear motion stage with the active RFC mechanism is built and

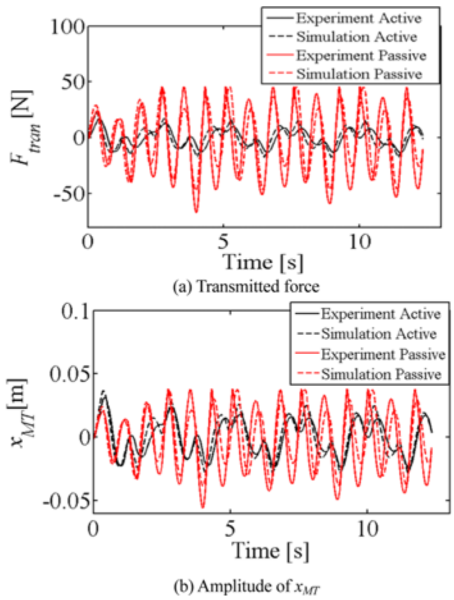

Fig. 14 Simulations and Experiments of passive and active RFC's with T_r = 0.2769 s and T_{dw} = 0.8571 s

shown in Fig. 12. Specifications of the linear motion stage and the active coil in the stage are summarized in Table 5. Power-PMAC motion controller is used for both mover and active coils. The magnet track motion is measured with hall sensor array.[16] The linear motion stage is used for both the passive and the active RFC since fixed P gain means the passive RFC and adjustable P gain means the active RFC. In addition, the transmitted force of both RFC's is calculated by Eq. (15).

Fig. 13 shows experimental results on transmitted force and magnet track motion of both RFC's, which matches well with simulation results of Fig. 11. Experiments are performed with keeping T_r = 0.2769 s and changing the dwell time from 0.2 to 2 s. The transmitted force of the active RFC is much smaller than that of the passive RFC satisfying the requirement of the magnet track motion.

Fig. 14 shows comparisons of simulation and experiments on transmitted force and magnet track motion of both RFC's with T_{dw} = 0.8571 s. Simulations show quite good match with experiments. In this case, transmissibility of the active RFC is 20% while that of the passive RFC is 82.5%. Furthermore, magnet track motion of the active RFC is smaller than that of the passive RFC.

7. Conclusion

In this paper, we develop a fuzzy-P controller of an active RFC mechanism to automatically tune the gain against variation of motion profiles. First, frequency components of motion profiles for a linear motion stage are analyzed and performances of the passive RFC mechanism are approximately evaluated using the motion profile analysis. An active RFC mechanism with an additional control coil is introduced to overcome limitation of the passive RFC mechanism and a fuzzy rule is proposed to automatically tune P controller of the active RFC mechanism according to variations of the motion profile. Simulations and experiments are performed to show the effectiveness of the proposed fuzzy rule for automatically tuning the P control gains of the active RFC mechanism.

ACKNOWLEDGEMENT

This research was supported by Basic Science Research Program through the National Research Foundation of Korea (NRF) funded by the Ministry of Education, Science and Technology (NRF-2013R1A1 A2010764) and supported by the MSIP (Ministry of Science, ICT & Future Planning), Korea, under the C-ITRC (Convergence Information Technology Research Center) (IITP-2015-H8601-15-1001) supervised by the IITP (Institute for Information & communications Technology Promotion).

REFERENCES

1. Tseng, Y. T. and Liu, J. H., “High-Speed and Precise Positioning of an X-Y Table,” Control Engineering Practice, Vol. 11, No. 4, pp. 357-365, 2003.
2. ASML, “TWINSCAN NXT:1960Bi,” http://www.asml.com/asml/show.do?lang=EN&ctx=46772&dfp_product_id=7414 (Accessed 15 APR 2015)
3. Cho, K. J., Choi, D. S., and Ahn, H. J., “Mechanism and Control of Reaction Force Compensation of Xy Linear Motion Stage System,” Transactions of the Korean Society of Mechanical Engineers A, Vol. 35, No. 6, pp. 599-607, 2011.
4. You, Y. H. and Ahn, H. J., “A Passive Reaction Force Compensation (RFC) Mechanism for a Linear Motor Motion Stage,” Int. J. Precis. Eng. Manuf., Vol. 15, No. 5, pp. 797-801, 2014.
5. Nguyen, D. C. and Ahn, H. J., “Dynamic Analysis and Iterative Design of a Passive Reaction Force Compensation Device for a Linear Motor Motion Stage,” Int. J. Precis. Eng. Manuf., Vol. 15, No. 11, pp. 2367-2373, 2014.
6. Galburt, D. N., “Method, System, and Apparatus for Management of Reaction Loads in a Lithography System,” US Patent, No. 6784978B2, 2004.
7. Poon, A. K. T., Kho, L. W. F., Yang, P. H., and Chang, P.-W., “Modular Stage with Reaction Force Cancellation,” US Patent, No. 6917412B2, 2005.
8. Zhang, P., “Advanced Industrial Control Technology,” Elsevier, Chap. 7, p. 293, 2010.
9. Precup, R. E. and Hellendoorn, H., “A Survey on Industrial Applications of Fuzzy Control,” Computers in Industry, Vol. 62, No. 3, pp. 213-226, 2011.
10. Zhen-Yu, Z., Tomizuka, M., and Isaka, S., “Fuzzy Gain Scheduling of PID Controllers,” IEEE Transactions on Systems, Man and Cybernetics, Vol. 23, No. 5, pp. 1392-1398, 1993.
11. Zheng, F., Wang, Q. G., Lee, T. H., and Huang, X., “Robust PI Controller Design For Nonlinear Systems Via Fuzzy Modeling Approach,” IEEE Transactions on Systems, Man and Cybernetics, Part A: Systems and Humans, Vol. 31, No. 6, pp. 666-675, 2001.
12. Güzelkaya, M., Eksin, I., and Yeºil, E., “Self-Tuning of PID-Type Fuzzy Logic Controller Coefficients Via Relative Rate Observer,” Engineering Applications of Artificial Intelligence, Vol. 16, No. 3, pp. 227-236, 2003.
13. Li, H. and Gupta, M. M., “Fuzzy Logic and Intelligent Systems,” Springer Science & Business Media, Chap. 4, p. 85, 1995.
14. Van, M., Kang, H. J., and Suh, Y. S., “A Novel Fuzzy Second-Order Sliding Mode Observer-Controller for a T-S Fuzzy System with an Application for Robot Control,” Int. J. Precis. Eng. Manuf., Vol. 14, No. 10, pp. 1703-1711, 2013.
15. Mathworks Inc., “Fuzzy Logic Toolbox™ User’s Guide,” 2014.
16. Ahn, H. J. and Kim, K. R., “2D Hall Sensor Array for Measuring the Position of a Magnet Matrix,” Int. J. Precis. Eng. Manuf.-Green Tech., Vol. 1, No. 2, pp. 125-129, 2014.